

## Model for the structural changes occurring at low temperatures in PdD<sub>x</sub>.

### II. Extension to lower concentrations

O. Blaschko, P. Fratzl, and R. Klemencic

*Institut für Experimentalphysik der Universität Wien Strudlhofgasse 4, A-1090 Wien, Austria*

*and Physikinstitut, Forschungszentrum Seibersdorf A-2444 Seibersdorf, Austria*

(Received 21 July 1981)

The concept of "mixed" microdomains presented in a previous paper for the description of the complicated diffuse intensity contours occurring in PdD<sub>x</sub> at low temperatures for  $x > 0.71$  has been extended to describe the diffuse scattering at lower concentrations, i.e.,  $x$  near 0.65. A diffuse neutron scattering experiment in PdD<sub>0.69</sub> is presented and the results in this intermediate-concentration range can easily be explained in the framework of the extended model. The model shows that the simple isointensity contours at lower concentrations can be described by "mixed" microdomains whose components are cells having a (100) mirror plane. The transition to the complicated contours for  $x > 0.71$  occurs when in the composition of the "mixed" domain the contribution of cells asymmetric relative to the (100) plane is progressively increased at higher concentrations.

### I. INTRODUCTION

Recent neutron scattering investigations have shown the existence of different ordering processes in nonstoichiometric PdD<sub>x</sub> at low temperatures.<sup>1-5</sup> For all concentrations investigated between  $x = 0.64$  and 0.78 a broad diffuse intensity around the  $1\frac{1}{2}0$  reciprocal-lattice point is observed.<sup>2-5</sup> For lower deuterium concentrations, i.e.,  $x = 0.64, 0.67$  the diffuse intensity is well centered at the  $1\frac{1}{2}0$  point and after cooling down below 50 K a superlattice reflection appears at the  $1\frac{1}{2}0$  point, increases in intensity and becomes narrower with time.<sup>2,3</sup> The ordered state in this low-concentration region has been characterized by an  $I4_1/amd$  structure, stoichiometric for 50% D.<sup>3</sup> For higher concentrations, i.e.,  $x > 0.71$ , however, the structural features are completely different: the diffuse scattering shows maxima shifted away from the  $1\frac{1}{2}0$  point, e.g., in PdD<sub>0.75</sub> a maximum is located at  $1.140.480$ .<sup>4</sup> Moreover, for  $x > 0.76$  after some aging time a superlattice reflection appears at the  $\frac{4}{5}\frac{2}{5}0$  point, indicating the presence of a long-range ordered state, which has been described by an interstitial Ni<sub>4</sub>Mo structure.<sup>1,5</sup> The short-range ordered state for  $x > 0.71$ , creating the complicated isointensity contours, has been described in a previous paper<sup>6</sup> (hereafter referred to by I) by "mixed" microdomains consisting of cells with different ordered structures of the Ni<sub>n</sub>Mo type.

In the present paper we have tried to connect the qualitatively different results in PdD<sub>x</sub> between the low- and the high-concentration region. Therefore we have measured a PdD<sub>x</sub> sample with an intermedi-

ate concentration of  $x = 0.69$  and the results are presented in Sec. III. Furthermore, in view of the present experimental results and using some concepts of (I) we have developed a qualitative model which is able to describe the structural features producing the transition to the ordering process occurring at lower concentrations (Sec. IV).

### II. EXPERIMENTAL

The neutron scattering experiment was carried out on the spectrometer D7 of the high flux reactor in Grenoble. The incident wavelength was 0.314 nm and the second-order contamination was suppressed by time-of-flight techniques. The sample with a [D]/[Pd] concentration of  $0.690 \pm 0.001$  was a cylindrical single crystal of Pd with a  $\langle 001 \rangle$  orientation, a diameter of 6 mm and a length of 20 mm. The crystal was loaded with deuterium from the gas phase and sealed finally by a copper film. After loading, the mosaic spread was 0.9°. The sample was mounted into a cryostat, cooled down to the selected temperature, and annealed for several hours, before starting the measurements. The diffuse intensity distribution around the  $1\frac{1}{2}0$  reciprocal-lattice point was determined first at 60, 50, and 40 K and then at 80 K.

### III. RESULTS

The diffuse intensity distribution measured at 60, 50, and 40 K are depicted as isointensity contours in Figs. 1(a), 1(b), and 1(c), respectively. The intensity

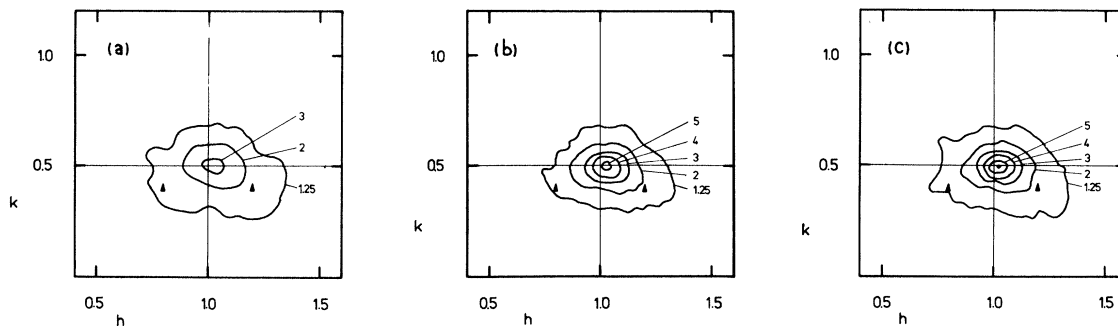


FIG. 1. Isointensity contours in the  $(hk0)$  plane of reciprocal space measured by neutron scattering from a  $\text{PdD}_{0.69}$  single crystal at (a)  $T = 60$  K, (b)  $T = 50$  K, and (c)  $T = 40$  K. The triangles indicate the positions  $\frac{4}{5}\frac{2}{5}0$  and  $\frac{6}{5}\frac{2}{5}0$ .

distributions show in  $\text{PdD}_{0.69}$  a maximum much nearer the  $1\frac{1}{2}0$  point than in  $\text{PdD}_{0.71}$ ,<sup>5</sup> but which is still shifted away from the exact  $1\frac{1}{2}0$  position. For 60 and 50 K the center of the distribution is located near the  $1.040.50$  point, but for 40 K the maximum approaches the  $1\frac{1}{2}0$  point, e.g., the center of the contour line 5 is now at  $1.020.50$ .

The temperature dependence of the diffuse intensity is shown in more detail in Fig. 2, which depicts a scan through the center of the distribution at different temperatures. From 80 to 60 K the peak increases by 60% but without changing its width. From 60 to 50 K a strong intensity increase is connected with a narrowing of the linewidth but without any appreciable change within the errors in the peak posi-

tion. Between 50 and 40 K a further intensity increase is observed, which is asymmetric in relation to the peak shape at 50 K and which consequently shifts the peak at 40 K to the  $1.020.50$  point. The inset of Fig. 2 shows the intensity difference between the scans at 50 and 40 K and reveals the presence of a peak, much narrower than the previous intensity distributions and located relatively well at the  $1\frac{1}{2}0$  point.

The time dependence of the diffracted intensity was checked by repeating one scan through the center of the distribution after having finished the measurement. At 40 K we found an increase of only  $3.5 \pm 1\%$  between 14 and 33 h after reaching 40 K, and at 50 K,  $2.5 \pm 1\%$  between 11 and 20 h.

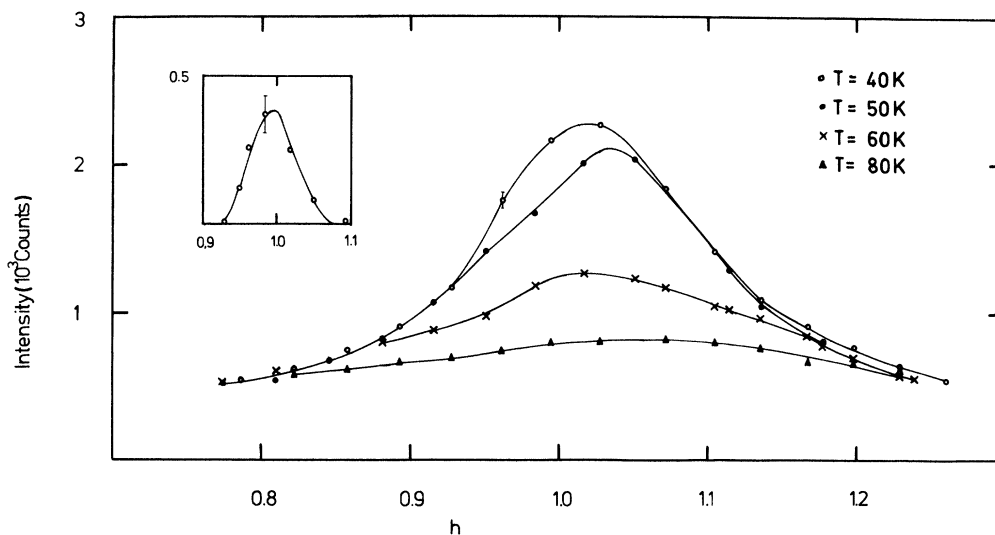


FIG. 2. Scan through the center of the diffuse intensity distribution along the line  $\langle h, 0.5, 0 \rangle$  at  $\blacktriangle T = 80$  K,  $\times T = 60$  K,  $\bullet T = 50$  K, and  $\circ T = 40$  K. The inset shows the subtraction of the measured intensity at 50 K from that at 40 K.

#### IV. STRUCTURAL MODEL FOR THE INTERMEDIATE CONCENTRATIONS

The results for  $\text{PdD}_{0.69}$  show some features of the diffuse scattering, which have not been observed before. First, the simple shape of the intensity distribution contrasts with the complicated iso-intensity contours observed at higher concentrations, i.e., for  $x > 0.71$  and has some similarity with the results in  $\text{PdD}_{0.64}$  and  $\text{PdD}_{0.67}$ . The center of the distribution, however, is shifted somewhat away from the  $1\frac{1}{2}0$  point but this displacement is much smaller than that of the maxima observed for  $x > 0.71$ .

Furthermore, for lower concentrations, the superlattice reflection at the  $1\frac{1}{2}0$  point seems to develop continuously out of the short-range order by intensity increase and a consequent narrowing of the linewidth.<sup>3</sup> For  $\text{PdD}_{0.69}$  a similar behavior has been found, but for intensity centered at the  $1.040.50$  point, and at 40 K an additional intensity well located at the  $1\frac{1}{2}0$  point appears, which can be described by a narrow peak (see inset of Fig. 2).

Therefore it appears that the diffuse scattering in  $\text{PdD}_{0.69}$  has some characteristics which have been found at lower concentrations, and some others, which have been observed at higher concentrations.

The short-range order in  $\text{PdD}_x$ , for  $x > 0.71$  has been explained in (I) by "mixed" microdomains consisting of cells of the  $\text{Ni}_n\text{Mo}$  type, where a simple distortion of the D atoms towards the vacant sites accounts for the observed intensity asymmetry relative to a (100) reciprocal plane. The structure of the cells  $\text{Ni}_n\text{Mo}$  ( $n = 1, 2, 3$ ) are shown in Fig. 1 of (I). For the concentration range below 70% a further "mosaic" cell has to be added to the structures  $\text{Ni}_n\text{Mo}$  ( $n = 1, 2, 3$ ). It is derived from the structure  $\text{NiMo}$  (concentration = 50%) of symmetry  $I4_1/amd$ , which is represented in Fig. 3. The  $\text{NiMo}$  structure exhibits a sequence of two filled and two vacant

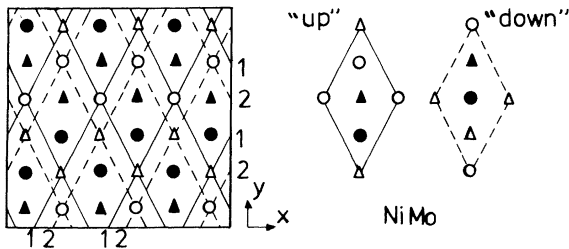


FIG. 3. Projection on a (001) plane of  $\text{NiMo}$  ( $I4_1/amd$ ) structure and the unit cell (in two positions). Filled symbols represent D atoms, open symbols vacancies; circles are corresponding to level 0 and triangles to level  $\frac{1}{2}$ . With full and broken lines are indicated the two families of  $\text{Ni}_3\text{Mo}$  cells easily superposable on  $\text{NiMo}$  structure.

(420) planes. The two vacant planes are indicated by full (plane 1) and broken (plane 2) lines. If one introduces a D atom on a vacant site of plane 1 one gets a  $\text{Ni}_3\text{Mo}$  cell enclosed by planes of type 2 and vice versa. This shows the great similarity between the structure  $\text{NiMo}$  and the two families of  $\text{Ni}_3\text{Mo}$  cells. Especially they are characterized by a symmetry relative to a (100) plane which  $\text{Ni}_2\text{Mo}$  and  $\text{Ni}_4\text{Mo}$  do not possess.  $\text{NiMo}$  and  $\text{Ni}_3\text{Mo}$  cells can be easily combined to a mixed domain. Therefore by mixing  $\text{NiMo}$  cells in the two positions "up" and "down" (see Fig. 3) and  $\text{Ni}_3\text{Mo}$  cells of the two families, it is possible to obtain the mean structure represented in Fig. 4<sup>7</sup> by its unit cell. This structure produces intensity at the  $1\frac{1}{2}0$  point and not at 100 and its average concentration is  $\frac{1}{2} + \Delta c$ , which accounts for the long-range order observed at low concentrations ( $x = 0.64$ ,  $x = 0.67$ ). Because of symmetry such a "mixed" structure has no average atomic displacement, i.e.,  $\langle u \rangle = 0$ , if the same tendency of the D atom to be displaced toward the vacant site is assumed, as found in (I) for higher concentrations.

The structure of Fig. 4 can also be understood in a different manner: By mixing equally  $\text{NiMo}$  cells "up" and "down" (see Fig. 3) one obtains the cell of Fig. 4 with  $\Delta c = 0$ . Then by distributing atoms equally over the vacant sites one obtains exactly the structure represented in Fig. 4 (when the macroscopic D concentration is  $\frac{1}{2} + \Delta c$ ). This establishes the connection between the model of a highly disturbed  $I4_1/amd$  structure<sup>3</sup> and the concept of mixed microdomains.

When the average concentration is increased towards higher  $x$  values,  $\Delta c$  increases and the average structure loses contrast. Moreover the probability for the local occurrence of less symmetric higher con-

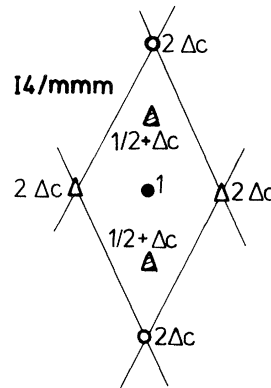


FIG. 4. Unit cell of average structure  $I4/mmm$  with macroscopic concentration  $\frac{1}{2} + \Delta c$ . Circles mean level 0 and triangles level  $\frac{1}{2}$ . The value of the site occupation operator (De Fontaine, Ref. 7) for each lattice site in unit cell is indicated in the figure.

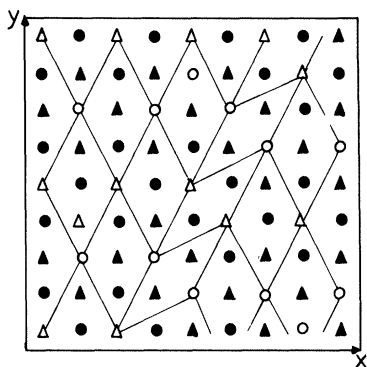


FIG. 5. A possible mixed microdomain with average concentration 0.69. The symbols are defined as in Fig. 3. This microdomain contains  $\text{Ni}_2\text{Mo}$  cells and produces a maximum of intensity near the  $1.040.50$  reciprocal-lattice point.

centrated cells is increased and therefore produces the transition to the “frustrated” state at higher concentrations (I). A possible configuration for the transition region is represented in Fig. 5 for an average concentration of  $x = 0.69$ .

The mixed structure (Fig. 5) still produces intensity near the  $1\frac{1}{2}0$  point, due to the dominating contribution of the  $\text{NiMo}$  and  $\text{Ni}_3\text{Mo}$  cells, but the inclusions of the  $\text{Ni}_2\text{Mo}$  type create a distortion of some D atoms in the  $[110]$  direction and therefore produce an average distortion per atom. As shown in (I) a distortion in the  $[110]$  direction induces an intensity asymmetry relative to the  $(100)$  plane, i.e., intensities lying on the right-hand side of the  $(100)$  plane in Fig. 1, are increased. Such distortion induced intensity asymmetry displaces the intensity around the  $1\frac{1}{2}0$  point toward higher  $h$  values. Consequently structures with  $\text{Ni}_2\text{Mo}$  inclusions, as shown, for instance, in Fig. 5, should describe the diffuse intensity in  $\text{PdD}_{0.69}$  and one would expect a peak in the vicinity of the  $1\frac{1}{2}0$  point but slightly shifted away, which has been observed indeed in the present experiment. We therefore conclude that microdomains with the average structure described in Fig. 4 should be responsible for the diffuse intensity contours observed in  $\text{PdD}_{0.69}$  at 60 and 50 K. The narrowing of the experimental linewidth is described in the microdomain concept by a growing of microdomains. The shift of the experimental contours toward the  $1\frac{1}{2}0$  point at 40 K comes out easily from the present model, when assuming that temperature decrease induces a further symmetrization of the mixed structure, i.e., a local transformation of the  $\text{Ni}_2\text{Mo}$  cells to the more symmetric  $\text{NiMo}$  and  $\text{Ni}_3\text{Mo}$  types, which reduces consequently the distortion of

the D lattice and creates intensity much nearer the  $1\frac{1}{2}0$  point.

## V. DISCUSSION

We have extended the “mixed” microdomain concept, explaining the diffuse scattering in  $\text{PdD}_x$ , at lower concentrations. The main new findings are: first a mixed domain with a highly symmetric structure consisting of cells of the  $\text{NiMo}$  and  $\text{Ni}_3\text{Mo}$  types describes the diffuse scattering at lower concentrations (Fig. 4). At intermediate concentrations, however, inclusions of less symmetric cells of the  $\text{Ni}_2\text{Mo}$  type produce an average distortion of the D lattice which shifts the  $1\frac{1}{2}0$  peak to higher  $h$  values, as found experimentally. Inversely, a local transformation of the  $\text{Ni}_2\text{Mo}$  cells to the more symmetric  $\text{NiMo}$  and  $\text{Ni}_3\text{Mo}$  structure cells reduces the average distortion and shifts the center of the diffuse scattering towards the  $1\frac{1}{2}0$  point, as found in  $\text{PdD}_{0.69}$  at 40 K.

A further concentration increase favors the occurrence of the higher concentrated  $\text{Ni}_4\text{Mo}$  cells producing therefore the mixed domain discussed in (I). The qualitative differences in the characteristics of the diffuse scattering contours at low and high concentrations, i.e., for  $x < 0.71$  a contour centered in the vicinity of the  $1\frac{1}{2}0$  point and for  $x > 0.71$  a complicated contour with maxima well outside the  $1\frac{1}{2}0$  point may therefore be understood in the framework of the “mixed” microdomains by the breakdown at higher concentrations of the easy possibility to form domains, consisting exclusively of highly symmetric cells of the  $\text{NiMo}$  and  $\text{Ni}_3\text{Mo}$  type.

Pairwise interaction energies for general fcc binary alloys have been computed previously by Richards and Cahn<sup>8</sup> and Allen and Cahn<sup>9,10</sup> taking into account second-neighbor interactions and ground-state structures have been determined. They find the following structures: for concentrations between 75 and 80% a two-phase region with  $\text{Ni}_4\text{Mo}$  and  $\text{Ni}_3\text{Mo}$ ; between 67 and 75% a two-phase region with  $\text{Ni}_3\text{Mo}$  and  $\text{Ni}_2\text{Mo}$  and below 67% a highly degenerate ground state.<sup>10</sup>

However the neutron scattering experiments<sup>1-6</sup> give no indication for the existence of two-phase regions in  $\text{PdD}_x$ . Nevertheless the description with “mixed” microdomains (I) uses cells of these ground-state structures, but in the present model the mixture is microscopic and without interface boundaries. Therefore the energy should not be far from that calculated by Allen and Cahn<sup>10</sup> but the structural features are quite different.

The structural features in  $\text{PdD}_x$  from  $x = 0.63$  to 0.78 may be described in the whole concentration region by the formation of “mixed” microdomains. At higher concentrations the mixed structure is composed mainly of cells of the  $\text{Ni}_n\text{Mo}$  (with  $n = 2, 3, 4$ )

structure, with different symmetries, which leads to a frustrated short-range ordered state. Only at concentrations higher than  $x = 0.76$  a long-range ordered  $\text{Ni}_4\text{Mo}$  phase can be nucleated. For lower concentrations  $x \leq 0.70$  the "mixed" domains are mainly composed by cells of the  $\text{NiMo}$  and  $\text{Ni}_3\text{Mo}$  type which have both the (100) mirror plane, allowing the formation of an "average" structure with symmetry  $I4_1/amd$  and lifting therefore the "frustration."

#### ACKNOWLEDGMENTS

We are highly indebted to Professor P. Weinzierl for his continuous support. This work was partially supported by the "Fonds zur Förderung der wissenschaftlichen Forschung in Österreich." We would like to thank the Institut Laue-Langevin for its hospitality.

---

<sup>1</sup>T. E. Ellis, C. B. Satterthwaite, M. H. Mueller, and T. O. Brun, *Phys. Rev. Lett.* **42**, 456 (1979).

<sup>2</sup>I. S. Anderson, C. J. Carlile, and D. K. Ross, *J. Phys. C* **11**, 381 (1978).

<sup>3</sup>I. S. Anderson, D. K. Ross, and C. J. Carlile, *Phys. Lett. A* **68**, 249 (1978).

<sup>4</sup>O. Blaschko, R. Klemencic, P. Weinzierl, O. J. Eder, and W. Just, *Solid State Commun.* **34**, 133 (1980).

<sup>5</sup>O. Blaschko, R. Klemencic, P. Weinzierl, O. J. Eder, and P.

von Blanckenhagen, *Acta Crystallogr. Sect. A* **36**, 605 (1980).

<sup>6</sup>O. Blaschko, P. Fratzl, and R. Klemencic, *Phys. Rev. B* **24**, 277 (1981).

<sup>7</sup>D. de Fontaine, *Solid State Phys.* **34**, 73 (1979).

<sup>8</sup>M. S. Richards and J. W. Cahn, *Acta Metall.* **19**, 1263 (1971).

<sup>9</sup>S. M. Allen and J. W. Cahn, *Acta Metall.* **20**, 423 (1972).

<sup>10</sup>S. M. Allen and J. W. Cahn, *Scr. Metall.* **7**, 1261 (1973).